Accepted Manuscript


# Structure-based discovery of novel 4,5,6-trisubstituted pyrimidines as potent covalent Bruton's tyrosine kinase inhibitors

Yi Zou, Jianhu Xiao, Zhengchao Tu, Yingyi Zhang, Kun Yao, Minghao Luo, Ke Ding, Yihua Zhang, Yisheng Lai

PII: S0960-894X(16)30498-X
DOI: http://dx.doi.org/10.1016/j.bmcl.2016.05.014
Reference: BMCL 23872

To appear in: *Bioorganic & Medicinal Chemistry Letters*

Received Date: 19 February 2016
Revised Date: 19 April 2016
Accepted Date: 4 May 2016

Please cite this article as: Zou, Y., Xiao, J., Tu, Z., Zhang, Y., Yao, K., Luo, M., Ding, K., Zhang, Y., Lai, Y., Structure-based discovery of novel 4,5,6-trisubstituted pyrimidines as potent covalent Bruton's tyrosine kinase inhibitors, *Bioorganic & Medicinal Chemistry Letters* (2016), doi: http://dx.doi.org/10.1016/j.bmcl.2016.05.014

This is a PDF file of an unedited manuscript that has been accepted for publication. As a service to our customers we are providing this early version of the manuscript. The manuscript will undergo copyediting, typesetting, and review of the resulting proof before it is published in its final form. Please note that during the production process errors may be discovered which could affect the content, and all legal disclaimers that apply to the journal pertain.

ACCEPTED MANUSCRIPT

# Structure-based discovery of novel 4,5,6-trisubstituted pyrimidines as potent covalent Bruton's tyrosine kinase inhibitors

Yi Zou[a,‡], Jianhu Xiao[a,‡], Zhengchao Tu[b,‡], Yingyi Zhang[a], Kun Yao[a], Minghao Luo[a] Ke Ding[b,*], Yihua Zhang[a], Yisheng Lai[a,*]

[a]*State Key Laboratory of Natural Medicines, Jiangsu Key Laboratory of Drug Discovery for Metabolic Diseases, Center of Drug Discovery, China Pharmaceutical University, Nanjing 210009, PR China*

[b]*Key Laboratory of Regenerative Biology and Institute of Chemical Biology, Guangzhou Institutes of Biomedicine and Health, Chinese Academy of Sciences, Guangzhou 510530, PR China*

**ABSTRACT**

A series of novel 4,5,6-trisubstituted pyrimidines were designed as potent covalent Bruton's tyrosine kinase (BTK) inhibitors based on the structure of ibrutinib by using a ring-opening strategy. Among these derivatives, compound **$I_1$** exhibited the most potent inhibitory activity with an $IC_{50}$ valve of 0.07 μM. The preliminary structure-activity relationship was discussed and the primary amino group at the C-4 position of pyrimidine was crucial for maintaining BTK activity. Furthermore, molecular dynamics simulations and binding free energy calculations were performed for three inhibitor-BTK complexes to determine the probable binding model, which provided a comprehensive guide for further structural modification and optimization.

**Keywords:** BTK, covalent kinase inhibitor, pyrimidine, structure-activity relationship, molecular dynamics simulation

‡These authors contributed equally to this work.

*Corresponding author. E-mail: yslai@cpu.edu.cn (Yisheng Lai); ding_ke@gibh.ac.cn (Ke Ding)

2016 Elsevier Ltd. All rights reserved.

ACCEPTED MANUSCRIPT

Bruton's tyrosine kinase (BTK), a member of the Tec family of non-receptor tyrosine kinases, plays a vital role in the B-cell signaling pathway linking cell surface B-cell receptor (BCR) stimulation to downstream intracellular responses. The expression and activity of BTK are critical to several key steps in the life cycle of B-lineage cells including proliferation, development, differentiation, survival, and apoptosis.[1,2] Ample evidence has indicated that the dysregulation of BTK is closely associated with the pathogenesis and development of various B-cell malignancies and autoimmune diseases, including rheumatoid arthritis, systemic lupus erythematosis, multiple sclerosis, B-cell lymphomas and leukemias, such as mantle cell lymphoma (MCL) and chronic lymphocytic leukemia (CLL).[3,4] Therefore, BTK has been considered as a potential therapeutic target for treating these diseases.

In recent years, many BTK inhibitors have been reported, which can be divided into two major classes, reversible and covalent irreversible ones, and some of them have been investigated in clinical trials.[5] Among these, covalent BTK inhibitors are a unique class of drugs, which form a covalent bond with a noncatalytic cysteine (Cys481) located at the rim of the ATP-binding pocket of BTK. This type of irreversible inhibitors has distinct characteristics compared with traditional reversible one, such as rapid onset of inhibition, greater potency, and longer duration of drug action.[6] Ibrutinib is a first-in-class irreversible inhibitor with subnanomolar against BTK ($IC_{50}$ = 0.5 nM),[7] and has been approved for the treatment of MCL,[8] CLL,[9] and Waldenström's macroglobulinemia (WM).[10] Subsequently, other fused pyrimidine-based covalent inhibitors of BTK, such as ONO-4059,[11] TM-71224,[12] and acalabrutinib,[13] were also quickly advanced into clinical trials for the treatment of B-cell malignancies and autoimmune disorders (Figure 1). Inspired by the pioneering work on these fused pyrimidines, we initiated docking simulations to investigate the interactions between ibrutinib and BTK, and found that the pyrazole moiety of ibrutinib didn't appear to make any visible interactions with the ATP-binding pocket directly, which provided new direction for development of novel covalent BTK inhibitors by the structural modification of this skeleton.

ACCEPTED MANUSCRIPT

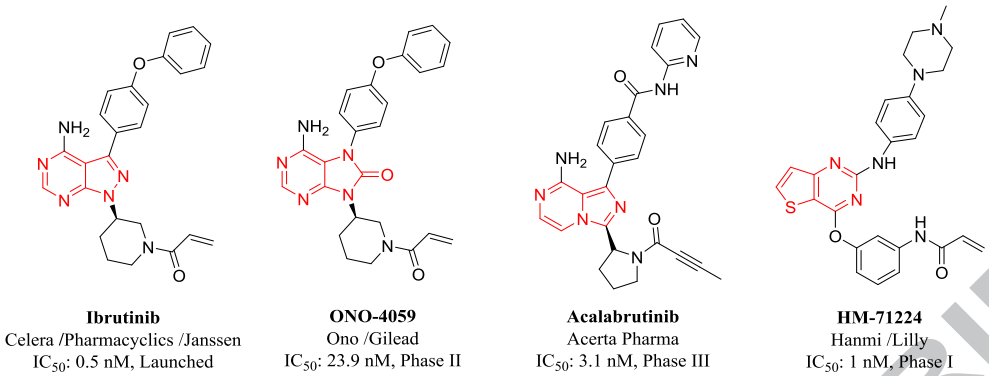


**Figure 1.** Representative fused pyrimidine-based covalent BTK inhibitors.

The protein structure, cocrystallized with an ibrutinib analogue **B43**,[14] was firstly carefully analyzed (PDB code: 3GEN). Besides, we performed docking simulations using Glide[15] in Schrodinger Suite with the default setting to investigate the interactions between ibrutinib and BTK. As predicted, docking simulations suggested that ibrutinib interacted with the active site in a fashion similar to compound **B43** (Figure 2). Briefly, the primary amine $NH_2$ formed two hydrogen bonds with the gatekeeper Thr474 hydroxyl and the backbone carbonyl of Glu475, the N-3 nitrogen of the pyrimidine ring interacted with the backbone NH of Met477 at the hinge region, and the diphenyl ether moiety occupied the hydrophobic pocket behind the Thr474 gatekeeper residue and displayed an edge-to-face aromatic interaction with Phe540. The sulfhydryl group of Cys481 of BTK was about 6 Å away from the acrylamide moiety at the head region of ibrutinib, which bound covalently to a cysteine residue proximal to the ATP-binding pocket of the kinase catalytic domain by Michael addition reaction *in vivo*. Meanwhile, we speculated that the pyrazolyl group of ibrutinib might act the role of maintaining its bioactive conformation merely as it didn't seem to make any visible interactions with the ATP-binding site.

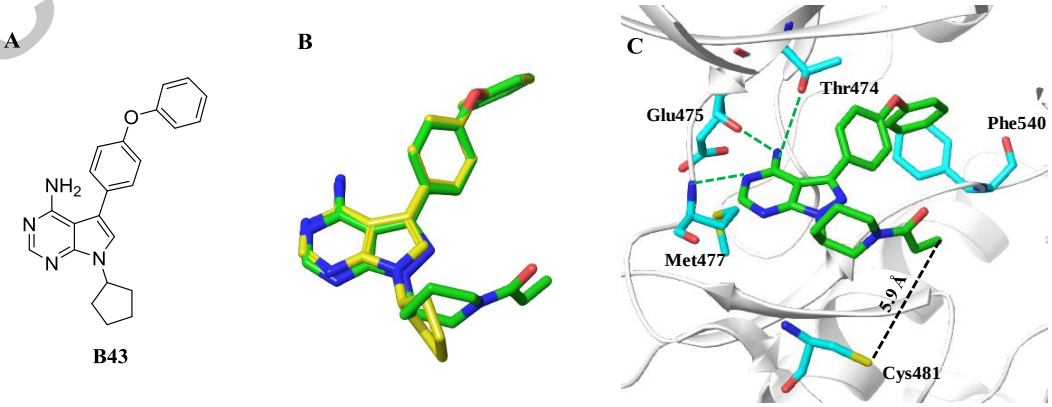


**Figure 2.** Docking mode of ibrutinib with BTK. (A) Chemical structure of **B43**. (B) Superposed docking poses of **B43** (yellow) and ibrutinib (green). (C) Docking pose of ibrutinib (green) with BTK. PDB ID:

ACCEPTED MANUSCRIPT

3GEN.

Based on the above analysis, we designed a series of novel pyrimidine-based BTK inhibitors by evolved the pyrazole ring of ibrutinib to 5-carbonyl and 6-amino using a ring-opening strategy (Figure 3).[16,17] We hoped that the active conformation could be retained through the formation of a pseudo-ring which was formed by intramolecular hydrogen bonding between carbonyl and amino group. The intramolecular hydrogen bond plays a unique role in drug design and discovery, as it could control the conformation of the molecules.[18,19] Two main factors were considered in the whole process of compound designing: the binding mode of the designed compounds should be overlapped well to that of ibrutinib, and their distances between Michael receptor and the sulfhydryl group of BTK Cys481 had to be similar to each other (around 6 Å).

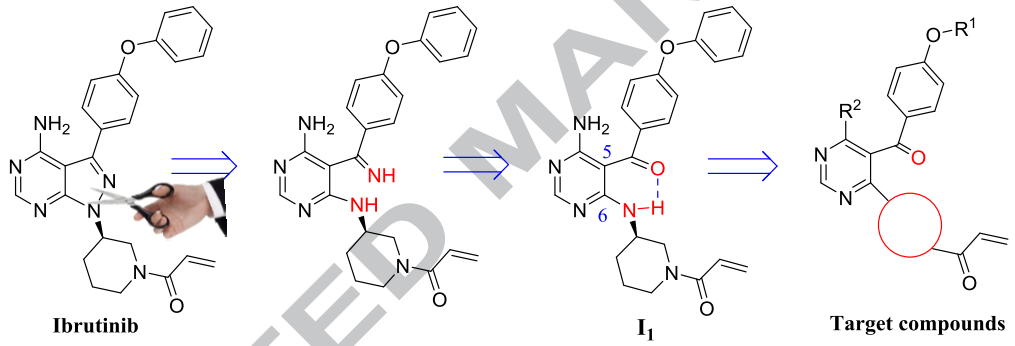


**Figure 3.** Design of 4,5,6-trisubstituted pyrimidine-based BTK inhibitors

After opening the pyrazole ring, compound **$I_1$** was firstly designed and synthesized (Figure 3). As can be seen from Figure 4A, docking simulations of the proposed compound **$I_1$** within the ATP binding site of BTK displayed almost the same binding mode to ibrutinib and the distance between Michael receptor and the sulfhydryl group of Cys481 of BTK was 5.5 Å. The preparation of compounds **$I_{1\text{-}9}$** was exemplified in Scheme 1. The commercially available pyrimidine-4,6-diol was subjected to Vilsmeier reaction with $POCl_3$ to give the aldehyde **1**, followed by oxidation with $NaH_2PO_4$ and $NaClO_2$ to obtain the corresponding carboxylic acid **2** in quantitative yields. Subsequent compound **2** was reacted with oxalyl chloride in anhydrous THF to give the corresponding acyl chloride which was used directly to assemble the key intermediate **3** by utilizing an intermolecular Friedel-Crafts acylation. The intermediates **3a-b** were then subjected to nucleophilic attack by (*R*)-1-Boc-3-aminopiperidine and substituted aliphatic amines to furnish compounds **5a-g**, respectively. After removing the Boc-protecting group of **5a-g**, the newly formed compounds were treated with acryloyl chloride to give the target

ACCEPTED MANUSCRIPT

compounds $\mathbf{I_{2-6}}$ and $\mathbf{I_{8-9}}$. Meanwhile, the intermediates **3a-b** were condensed successively with ammonia and (*R*)-1-Boc-3-aminopiperidine to generate compounds **8a-b**, followed by removal of the Boc-protecting group to give **9a-b** as intermediates. Finally, the desired products $\mathbf{I_1}$ and $\mathbf{I_7}$ were prepared via the reaction of **9a-b** and acryloyl chloride under an atmosphere of nitrogen.

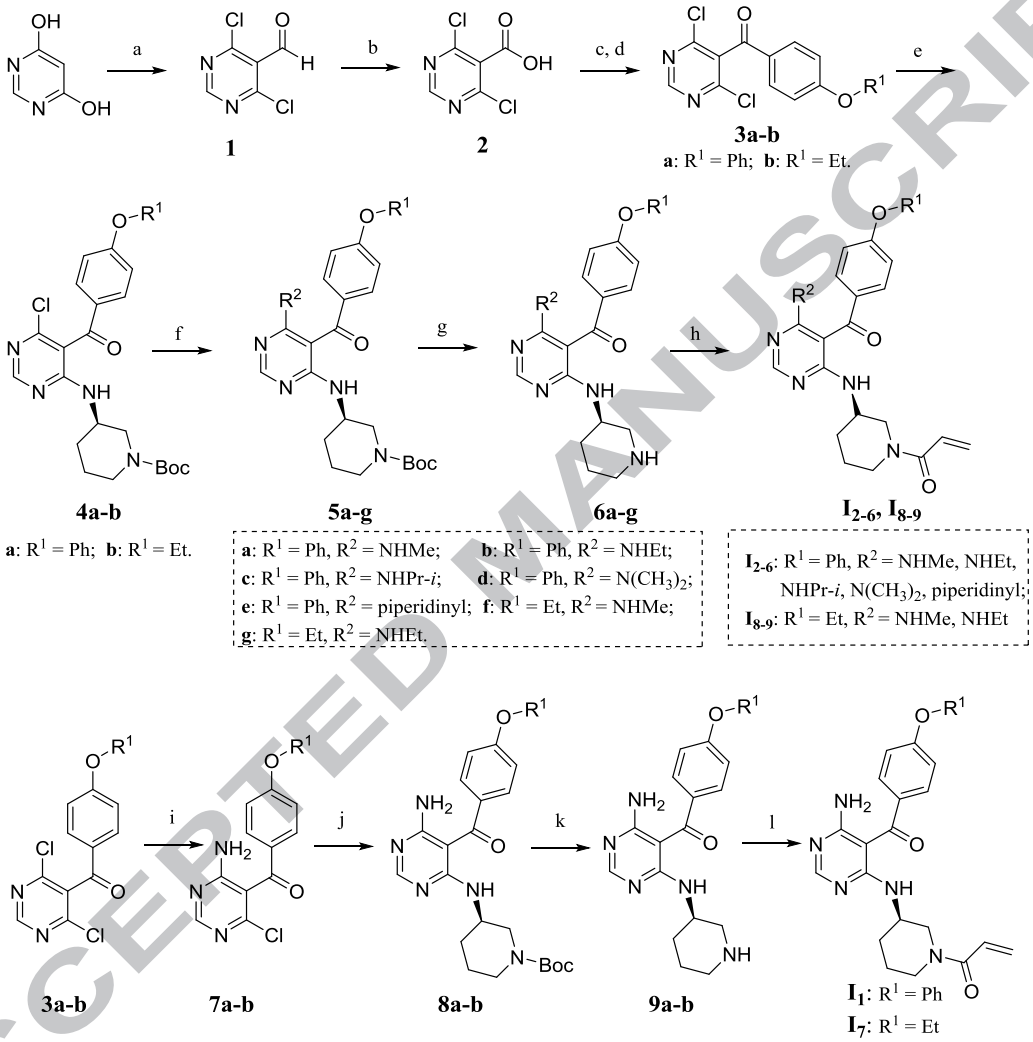


**Scheme 1.** General synthetic route to the target compounds $\mathbf{I_{1-9}}$. Reagents and conditions: (a) $POCl_3$, DMF, 0 $^oC$, 1 h; rt, 30 min; reflux, 3 h; (b) $NaH_2PO_4$, $NaClO_2$, *t*-BuOH/$H_2O$ (3/1, V/V), 0 $^oC$, 1 h; (c) $(COCl)_2$, DMF, anhydrous THF, rt, 4 h; (d) $AlCl_3$, anhydrous $CH_2Cl_2$, reflux, 3 h; (e) (*R*)-1-Boc-3-aminopiperidine, DIPEA, EtOH, rt, 24 h; (f) DIPEA, EtOH, reflux, 6 h; (g) TFA, anhydrous $CH_2Cl_2$, rt, 12 h; (h) Acryloyl chloride, anhydrous $CH_2Cl_2$, rt, 2 h; (i) $NH_3 \cdot H_2O$, EtOH, rt, 24 h; (j) (*R*)-1-Boc-3-aminopiperidine, DIPEA, EtOH, reflux, 72 h; (k) TFA, anhydrous $CH_2Cl_2$, rt, 12 h; (l) Acryloyl chloride, anhydrous $CH_2Cl_2$, rt, 2 h.

Visual inspection of docking result also revealed that the para position of substituted piperidine ring of compound $\mathbf{I_1}$ was closer to Cys481 when compared to the meta position (6.5 Å and 6.0 Å, respectively)

ACCEPTED MANUSCRIPT

(Figure 4B). We anticipated that the addition of Michael acceptor extending from the para position of this piperidine ring would yield substituents which also could directly interact with the sulfhydryl group of Cys481. Thus, compounds **II$_{1-8}$** were designed for this goal and the docking results indicated that the distance between Michael receptor and the sulfhydryl group of BTK Cys481 was 4.7 Å (Figure 4C). The general synthetic routes for the preparation of title compounds **II$_{1-8}$** were illustrated in Scheme 2 and the procedures were similar to that described above.

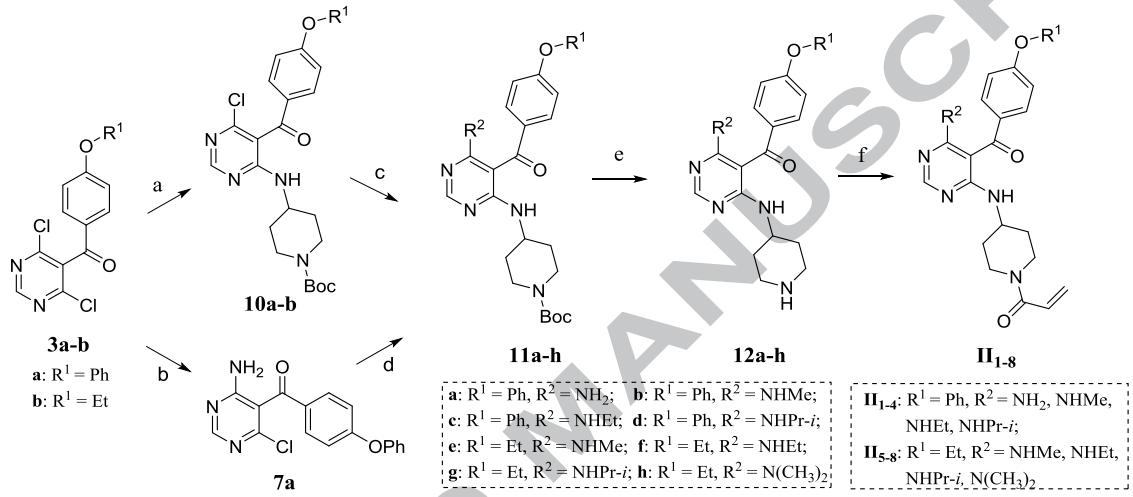


**Scheme 2.** General synthetic route to the target compounds **II$_{1-8}$** Reagents and conditions: (a) 1-Boc-4-aminopiperidine, DIPEA, EtOH, rt, 24 h; (b) DIPEA, EtOH, rt, 24 h; (c) DIPEA, EtOH, reflux, 6 h; (d) 1-Boc-4-aminopiperidine, DIPEA, EtOH, reflux, 72 h; (e) TFA, anhydrous $CH_2Cl_2$, rt, 12 h; (f) Acryloyl chloride, anhydrous $CH_2Cl_2$, rt, 2 h.

Subsequently, compounds **III$_{1-8}$** with tertiary amino group at C-6 were designed to inspect whether the whole active conformation could be remained when they cannot form the intramolecular hydrogen bond as we predicted (Figure 4D). Modeling also exhibited a good overlay of compound **III$_1$** with ibrutinib and the distance between Michael receptor and the sulfhydryl group of BTK Cys481 was still within the ideal range (5.5 Å). As shown in Scheme 3, compounds **14a-h** were obtained via nucleophilic attack by substituted aliphatic amine or ammonia and piperazine in sequence, followed by the treatment with acryloyl chloride to furnish **III$_{1-8}$** as the target compounds.

ACCEPTED MANUSCRIPT

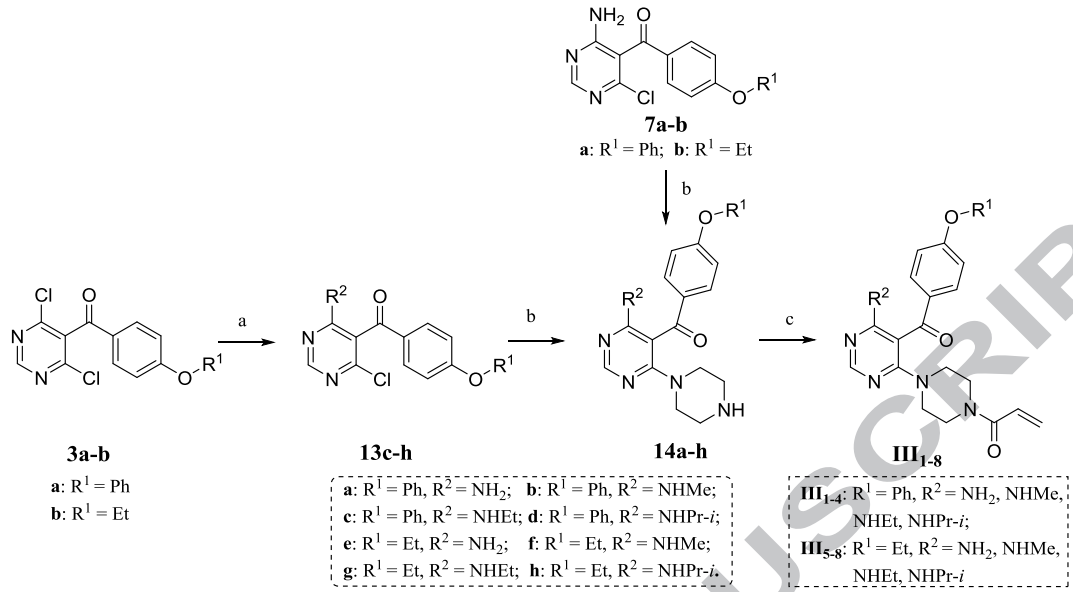


**Scheme 3.** General synthetic route to the target compounds $\mathbf{III_{1-8}}$. Reagents and conditions: (a) $RNH_2$, IPA, 0 $^oC$, 1 h; (b) Piperazine, EtOH, reflux, 4 h; (c) Acryloyl chloride, anhydrous $CH_2Cl_2$, rt, 2 h.

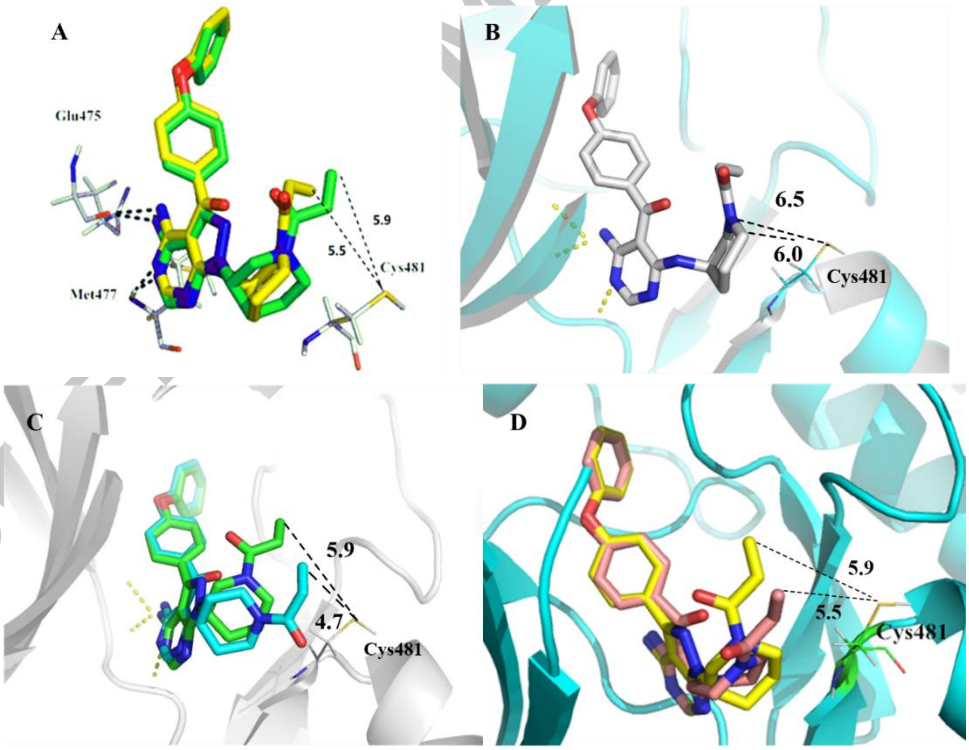


**Figure 4.** Docking mode of the target compounds with BTK. (A) Superimposition of the docking models of ibrutinib (green) and compound $\mathbf{I_1}$ (yellow); (B) The distances from the para and meta position of substituted piperidine ring of compound $\mathbf{I_1}$ to the sulfhydryl group of the targeted cysteine; (C) Superimposition of the docking models of ibrutinib (green) and compound $\mathbf{II_1}$ (yellow); (D) Superimposition of the docking models of ibrutinib (yellow) and compound $\mathbf{III_1}$ (pink).

ACCEPTED MANUSCRIPT

The target compounds **I-III** were evaluated for their inhibitory activity against BTK by Z-Lyte fluorescence resonance energy transfer method and ibrutinib was served as the reference compounds. As shown in Table 1, compounds with a primary amino group at the C-4 position turned out to be more effective for the BTK kinase inhibition without exception. When secondary amino, tertiary amino and even halogeno groups were installed at the C-4 position respectively, the resulting 4,5,6-trisubstituted pyrimidine derivatives displayed significantly lower potency against BTK kinase. These results indicated that the amino group at the C-4 position was critical to its inhibitory potency against BTK. Meanwhile, the linker moiety between Michael receptor and the pyrimidine scaffold had an impact on the distance to Cys481, which also played an important role in inhibition against BTK enzyme. It was observed that compound $\mathbf{I_1}$ with a 3-aminopiperidinyl linker displayed better activity compared to compounds $\mathbf{II_1}$ (4-aminopiperidinyl-linker) and $III_1$ (piperazinyl-linker). It was worth mentioning that compounds $\mathbf{III_1}$ and $\mathbf{III_5}$ were nearly equivalent to compound $\mathbf{II_1}$ with $IC_{50}$ values of 0.88 μM, 1.32 μM, and 1.07 μM, respectively. The results indicated that the lack of intramolecular hydrogen bonding may have little effect on the activity. This was most likely because its bioactive conformation was still maintained by the increase of the rigidity of the entire molecule compare to compounds **I-II** (Figure 4D). Furthermore, the $R^1$ group of the target compounds extended into the hydrophobic pocket was investigated. Surprisingly, replacement of the phenyl group in compound $\mathbf{I_1}$ by an ethyl group resulted in a substantial reduction in potency (compound $\mathbf{I_7}$ was 25-fold less active than $\mathbf{I_1}$). This was consistent with modeling studies from which it was evident that the phenyl ring sits in a hydrophobic pocket of BTK, forming an edge-to-face interaction with Phe540. These results indicated that the diphenyl ether group was optimal for BTK activity. Mass spectrometry experiment was further employed to assess the ability of a small molecule to form a covalent adduct with BTK. In this method, compound $\mathbf{I}_1$ (molecular mass, 443.2 Da) with the highest inhibitory activity against BTK was used to incubate with an aqueous solution of the catalytic domain of BTK (393-657). After analyzing with a Waters LC-MS system, we found that the peak was fully shifted compared with the mass of apo BTK kinase domain (molecular mass, 32814.8 Da), which obviously indicated that compound $\mathbf{I_1}$ was a covalent inhibitor of BTK (Figure S1 in the Supplementary Data).

ACCEPTED MANUSCRIPT

**Table 1.** Activities of 4,5,6-trisubstituted pyrimidines **I-III**.

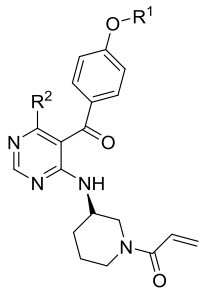

$\mathbf{I_{1-9}}$

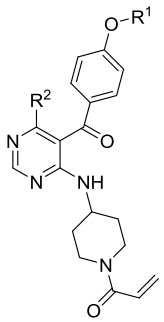

$\mathbf{II_{1-8}}$

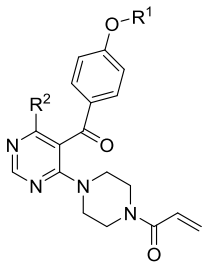

$\mathbf{III_{1-8}}$

| Compd. | $R^1$ | $R^2$ | Inhibitory rate [a] (%) | $IC_{50}$ [b] |
|---|---|---|---|---|
| **$I_1$** | Ph | $NH_2$ | 100.51 | 0.07 μM |
| **$I_2$** | Ph | $NHCH_3$ | 6.66 | nd |
| **$I_3$** | Ph | $NHCH_2CH_3$ | 18.24 | nd |
| **$I_4$** | Ph | $NHCH(CH_3)_2$ | 14.56 | nd |
| **$I_5$** | Ph | $N(CH_3)_2$ | 11.42 | nd |
| **$I_6$** | Ph | Piperidinyl | 15.67 | nd |
| **$I_7$** | $CH_2CH_3$ | $NH_2$ | 52.88 | 1.80 μM |
| **$I_8$** | $CH_2CH_3$ | $NHCH_3$ | 10.27 | nd |
| **$I_9$** | $CH_2CH_3$ | $NHCH_2CH_3$ | 0 | nd |
| **$II_1$** | Ph | $NH_2$ | 78.14 | 1.07 μM |
| **$II_2$** | Ph | $NHCH_3$ | 10.61 | nd |
| **$II_3$** | Ph | $NHCH_2CH_3$ | 0 | nd |
| **$II_4$** | Ph | $NHCH(CH_3)_2$ | 1.20 | nd |
| **$II_5$** | $CH_2CH_3$ | $NHCH_3$ | 0 | nd |
| **$II_6$** | $CH_2CH_3$ | $NHCH_2CH_3$ | 6.81 | nd |
| **$II_7$** | $CH_2CH_3$ | $NHCH(CH_3)_2$ | 8.69 | nd |
| **$II_8$** | $CH_2CH_3$ | $N(CH_3)_2$ | 9.80 | nd |
| **$III_1$** | Ph | $NH_2$ | 93.21 | 0.88 μM |
| **$III_2$** | Ph | $NHCH_3$ | 8.14 | nd |
| **$III_3$** | Ph | $NHCH_2CH_3$ | 17.53 | nd |
| **$III_4$** | Ph | $NHCH(CH_3)_2$ | 48.54 | nd |
| **$III_5$** | $CH_2CH_3$ | $NH_2$ | 87.67 | 1.32 μM |
| **$III_6$** | $CH_2CH_3$ | $NHCH_3$ | 11.87 | nd |
| **$III_7$** | $CH_2CH_3$ | $NHCH_2CH_3$ | 6.43 | nd |
| **$III_8$** | $CH_2CH_3$ | $NHCH(CH_3)_2$ | 24.04 | nd |
| Ibrutinib | | | 100.13 | 0.64 nM |

[a] Inhibitory rate at 10 μM.

[b] Enzyme $IC_{50}$ values are averages of two or more experiments. nd: not determined

ACCEPTED MANUSCRIPT

Compared with the standard docking studies, molecular dynamics (MD) is a computer simulation method for studying the physical movements of atoms and molecules, giving a view of the dynamical evolution of the system.[20] To investigate the effect on activity made by our ring-opening operation, three prime-refined complexes, derived directly from the docking-based modeling of BTK and its binding with ibrutinib, compound **$I_1$** and compound **$III_5$**, were selected to conduct the molecular dynamics simulation, respectively. Binding free energy calculation and two distance parameters analysis (the distance between two non-hydrogen atoms that can form hydrogen bond and the distance between Michael receptor of the inhibitor and the sulfhydryl group of BTK Cys481) will provide the detailed information about the differences between each complex. Root-mean-square deviation (RMSD) of the backbone atoms of these complexes and root-mean-square fluctuations (RMSF) were calculated based on MD trajectory frames. For each BTK-inhibitor complex, after the MD simulation was finished, 10 snapshots from the equilibrium period of the MD trajectory with one snapshot for every 100 ps were extracted and subjected to binding free energy calculation.

The evolution of RMSD of each system during 10 ns and 15 ns MD simulations was profiled in Figure 5. For each complex, the protein-ligand system reached the converged stage early at about 2 ns. The backbone of receptor fluctuated around 0.25 nm, and the ligand changed in the range of 0.05-0.1 nm during the remaining simulation time, which showed the protein-ligand system reached the equilibrated and stable stage (Figure 5A, 5C and 5E). The macroscopic variables, including density, energy, pressure, and temperature, also showed the protein-ligand system reached the equilibrated and stable stage (Figure S2, S4 and S6 in the Supplementary Data). The RMSF plots were made to determine the flexibility of residues in the binding pocket during the simulation. Little changes were found on the conserved amino acid residues in the process of the simulation, like the hinge region (Thr474, Glu475 and Met477) and the hydrophobic region (Phe540), indicating that the ligand binding site was also kept in a stable conformation (Figure 5B, 5D and 5F). Residue Cys481 was kept at a moderate value and its distance to ibrutinib (vinyl β-C) was 0.53 ± 0.07 nm, which bound covalently to ibrutinib actually. Vinyl β-C of Compound **$I_1$** had the shortest distance to residue Cys481 (0.42 ± 0.05 nm), while compound **$III_5$** showed the longest distance to it (0.63 ± 0.04 nm), which probably accounted for the significant difference in inhibitory activity against BTK between them. Besides the differences made by the tendency for covalent binding, hydrogen bond interactions with the binding pocket also played an important role. From the results of hydrogen bond distance analysis, all three compounds formed stable hydrogen bonds with the

ACCEPTED MANUSCRIPT

hinge region residues, which were considered to be the key residues for binding with the inhibitors. The primary amino group of these compounds were strongly hydrogen-bonded with the carbonyl oxygen at the backbone of residue Glu475 and the distance increased gradually from 0.31 ± 0.01 nm for BTK-ibrutinib and BTK-compound **$I_1$** binding, to 0.33 ± 0.02 nm for BTK-compound **$III_5$** interaction. The average distance between the 3-nitrogen atom on the pyrimidine skeleton of the inhibitor and the nitrogen atom on the backbone of residue Met477 was 0.32 ± 0.01 nm for BTK-ibrutinib binding, 0.32 ± 0.01 nm for BTK-compound **$I_1$** binding and 0.31 ± 0.04 nm for BTK-compound **$III_5$** binding. Compared to the BTK-compound **$I_1$** (0.49 ± 0.06 nm) and BTK-compound **$III_5$** complexes (0.51 ± 0.05 nm), the BTK-ibrutinib complex (0.37 ± 0.05 nm) had the shortest distance between the nitrogen atom on the amine group of the inhibitor to the side chain of residue Thr474, as tracked from the MD trajectories. These results suggested that even though the hydrogen-bond interaction between the inhibitor and residue Thr474 was relatively weaker than two other critical residues, it was of critical effect upon the inhibitory activity against BTK (Figure 6).

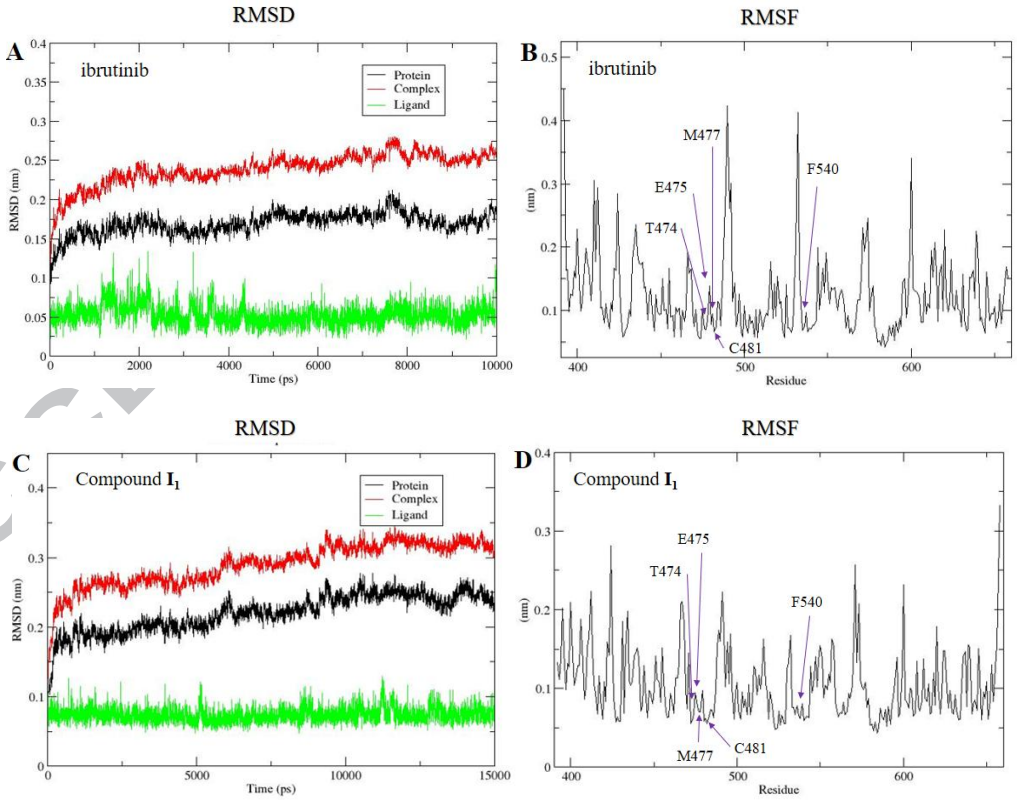

ACCEPTED MANUSCRIPT

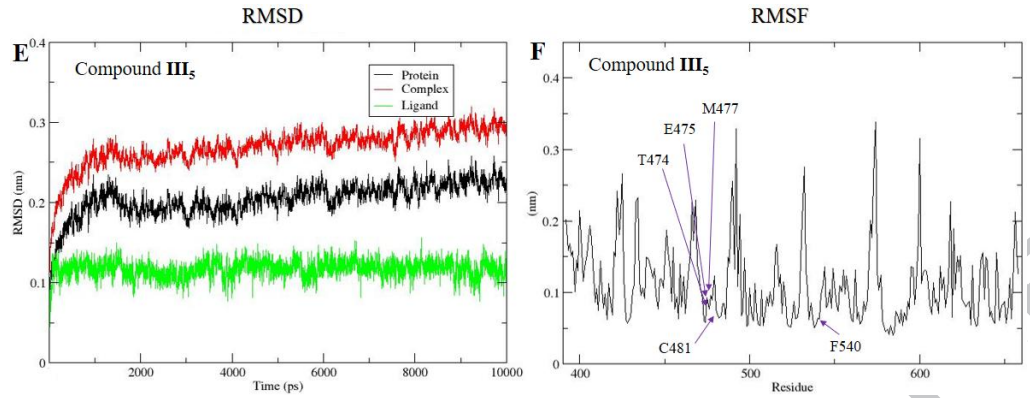


**Figure 5.** Stability examination for MD simulations. Tracked positional root-mean square deviation (RMSD) for backbone atoms of the binding structure of BTK binding with ibrutinib (A), compound **$I_1$** (C) and compound **$III_5$** (E) along with MD trajectories. Atomic fluctuations (RMSF) of BTK residue Cα atoms during MD trajectories (B) (D) (F).

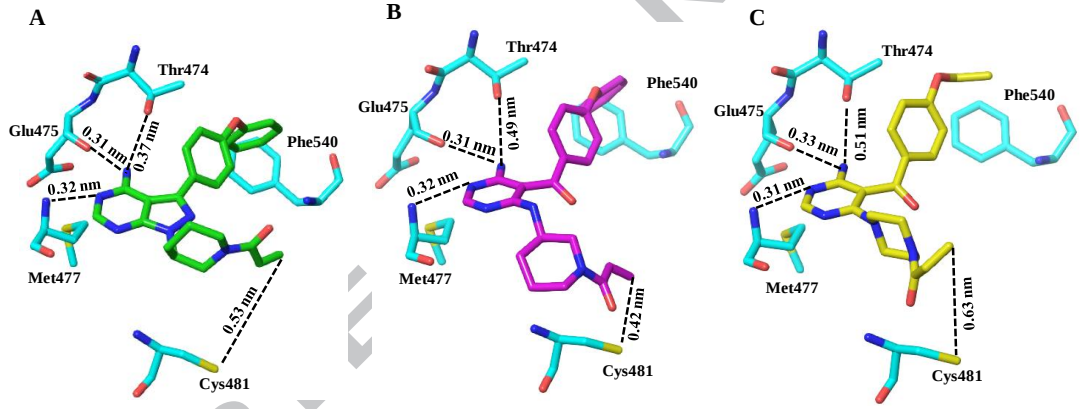


**Figure 6.** Intermolecular interactions in the prime-refined BTK-inhibior binding structure. Residues from BTK within 0.5 nm of inhibitor are labeled and shown in stick style (turquoise). The dashed line represents the averaged distance between non-hydrogen atoms of key residues of BTK and inhibitor based on the MD trajectory. (A) Ibrutinib is colored in green; (B) compound **$I_1$** is colored in purple; (C) compound **$III_5$** is colored in yellow.

Binding free energy was calculated for these compounds using MM/PBSA method[21,22] which was considered to reflect the binding affinity of the ligands (Figure 7). Overall, the calculated effective binding energies of the complex showed significant negative values, indicating the favorable protein-ligand interaction. Ibrutinib got more favorable $\Delta G_{bind}$ values than compounds **$I_1$** and **$III_5$**, indicating that ibrutinib got higher binding affinity with binding pocket. This was consistent with the activity differences between these three compounds and, thus, may be valuable for future computational design of new and potent BTK inhibitors.

ACCEPTED MANUSCRIPT

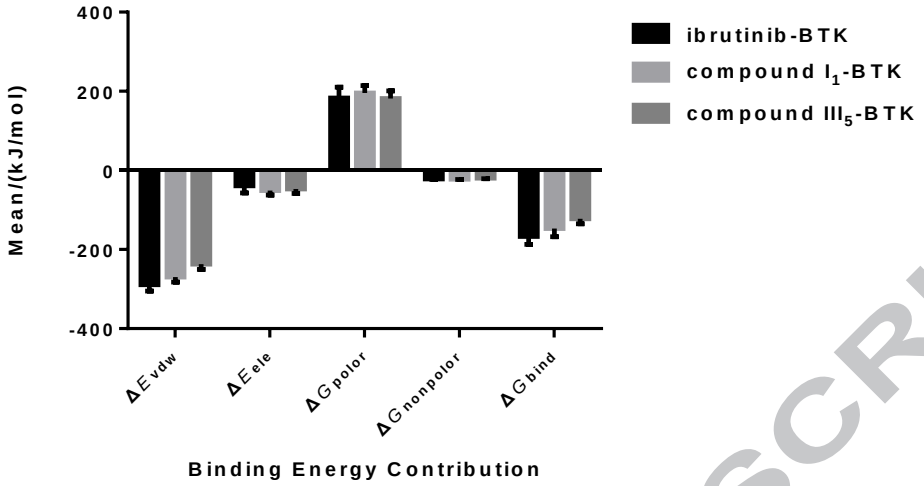


**Figure 7.** Binding free Energy calculated using MM-PBSA. Data are shown as mean ± standard error of the mean.

Furthermore, we utilized CovDock, a covalent docking program developed by Schrödinger,[23] to investigate the effect of covalent bonding during molecular modeling. This method consists of conventional noncovalent docking of the prereactive species, heuristic formation of the covalent attachment, and structural refinement of the covalently bound protein-ligand complex. We have extensively investigated the conformational differences of ibrutinib and compound **$I_1$** between covalent and non-covalent docking performances. The pose prediction assessment was based on the heavy atom RMSD between the covalent docking structure and non-covalent docking structure. Our results demonstrated that ibrutinib and compound **$I_1$** showed relatively lower RMSD values (0.61 Å and 0.53 Å, respectively). As can be seen from Figure 8, the fragments occupied at the hinge and hydrophobic region experienced little conformational change between covalent and non-covalent docking structure, so most of the important interactions between inhibitor and BTK still retained after covalent docking. The difference of RMSD value was prevailingly derived from the conformational change at the head region of ibrutinib and compound **$I_1$**, which might adjust their orientation to facilitate reaction for forming covalent bond to BTK protein.

ACCEPTED MANUSCRIPT

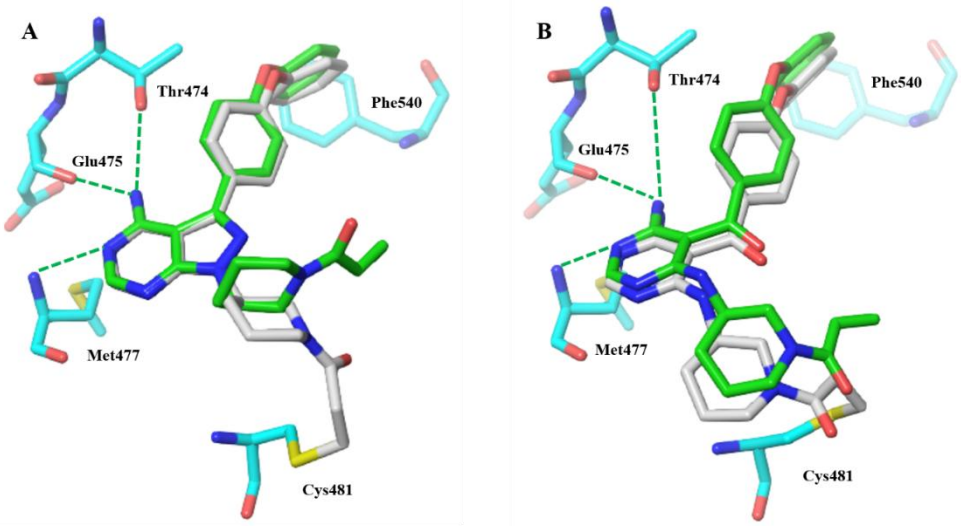


**Figure 8**. The comparison of the binding mode between the covalent (white) and non-covalent (green) docking structure. Residues from BTK within 0.5 nm of inhibitor are labeled and shown in stick style (turquoise). The green dotted line represents the hydrogen bonding interaction between inhibitors and BTK. (A) ibrutinib; (B) compound $\mathbf{I_1}$.

In conclusion, we have designed and synthesized three kinds of novel 4,5,6-trisubstituted pyrimidine derivatives based on the structure of ibrutinib using a ring-opening strategy in the present work. Among them, compound $\mathbf{I_1}$ showed the most potent inhibitory activity with an $IC_{50}$ valve of 0.07 μM and its covalent binding mechanism was proved by mass spectrometry experiment. The preliminary structure-activity relationship was disclosed and the primary amino group at the C-4 position of pyrimidine was crucial for maintaining its inhibitory potency against BTK. The subsequent 10 ns or 15 ns molecular dynamic simulations of the formerly mentioned protein-ligand complexes, viz., ibrutinib, compound $\mathbf{I_1}$ and compound $\mathbf{III_5}$ were done to probe the binding mode and the stability of predicted protein-ligand complexes, and assess the contributions to ligand binding and activity against BTK. The results of this study will facilitate the research and accelerate the discovery of novel BTK inhibitors with high activity and selectivity.

**Acknowledgments**

This research was supported by grants from the National Natural Science Foundation of China (No. 21472244), the Natural Science Foundation of Jiangsu Province (No. BK2011626), the Six Major Talent Peak Project of Jiangsu Province (No. 2011-YY-004), and the Fundamental Research Funds for the Central Universities (No. 2015021).

ACCEPTED MANUSCRIPT

**Supplementary data**

Supplementary data (chemistry methods, characterization, bioactivity test methods, molecular docking and molecular dynamic methods) associated with this article can be found, in the online version, at http://dx.doi.org/10.1016/j.bmcl.2016.xx.xxx.

**References and notes**


1. Rokosz, L. L.; Beasley, J. R.; Carroll, C. D.; Lin, T.; Zhao, J.; Appell, K. C.; Webb, M. L. *Expert Opin. Ther. Targets* **2008**, *12*, 883.
2. Kurosaki, T.; Hikida, M. *Immunol. Rev.* **2009**, *228*, 132.
3. De Weers, M.; Verschuren, M. C. M.; Kraakman, M. E. M.; Mensink, R. G. B.; Schuurman, R. K. B.; Dongen, J. J. M.; Hendriks, R. W. *Eur. J. Immunol*. **1993**, *23*, 3109.
4. 4Katz, F. E.; Lovering, R. C.; Bradley, L. A.; Rigley, K. P.; Brown, D.; Cotter, F.; Chessells J. M.; Levinsky R. J.; Kinnon C. *Leukemia* **1994**, *8*, 574.
5. Akinleye, A.; Chen, Y.; Mukhi, N.; Song, Y.; Liu, D. *J. Hematol. Oncol*. **2013**, *6*, 59.
6. Singh, J.; Petter, R. C.; Baillie, T. A.; Whitty, A. *Nat. Rev. Drug Discovery* **2011**, *10*, 307.
7. Pan, Z.; Scheerens, H.; Li, S. J.; Schultz, B. E.; Sprengeler, P. A.; Burrill, L. C.; Mendonca, R. V.; Sweeney, M. D.; Scott, K. C.; Grothaus, P. G.; Jeffery, D. A.; Spoerke, J. M.; Honigberg, L. A.; Young, P. R.; Dalrymple, S. A.; Palmer, J. T. *ChemMedChem* **2007**, *2*, 58.
8. Byrd, J. C.; Furman, R. R.; Coutre, S. E.; Flinn, I. W.; Burger, J. A.; Blum, K. A.; Grant, B.; Sharman, J. P.; Coleman, M.; Wierda, W. G.; Jones, J. A.; Zhao, W.; Heerema, N. A.; Johnson, A. J.; Sukbuntherng, J.; Chang, B. Y.; Clow, F.; Hedrick, E.; Buggy, J. J.; James, D. F.; O'Brien, S. *N. Engl. J. Med.* **2013**, *369*, 32.
9. Wang, M. L.; Simon, R.; Peter, M.; Andre, G.; Rebecca, A.; Kahl, B. S.; Wojciech, J.; Advani, R. H.; Romaguera, J. E.; Williams, M. E. *N. Engl. J. Med.* **2013**, *369*, 507.
10. Treon, S. P.; Tripsas, C. K.; Meid, K.; Warren, D.; Varma, G.; Green, R.; Argyropoulos, K. V.; Yang, G.; Cao, Y.; Xu, L.; Patterson, C. J.; Rodig, S.; Zehnder, J. L.; Aster, J. C.; Harris, N. L.; Kanan, S.; Ghobrial, I.; Castillo, J. J.; Laubach, J. P.; Hunter, Z. R.; Salman, Z.; Li, J.; Cheng, M.; Clow, F.; Graef, T.; Palomba, M. L.; Advani, R. H. *N. Engl. J. Med.* **2015**, *372*, 1430.
11. Yasuhiro, T.; Yoshizawa, T.; Birkett, J. T. P.; Kawabata, K. *Blood* **2013**, *122*, 5151.
12. Park, J.K.; Park, J.A.; Lee, Y.J.; Song, J.; Oh, J.I.; Lee, Y.-M.; Suh, K.H.; Son, J.; Lee, E.B. *Ann. Rheum. Dis*. **2014**, *73*, 355.
13. Byrd, J. C.; Harrington, B.; O'Brien, S.; Jones, J. A.; Schuh, A.; Devereux, S.; Chaves, J.; Wierda, W. G.; Awan, F. T.; Brown, J. R.; Hillmen, P.; Stephens, D. M.; Ghia, P.; Barrientos, J. C.; Pagel, J. M.; Woyach, J.; Johnson, D.; Huang, J.; Wang, X.; Kaptein, A.; Lannutti, B. J.; Covey, T.; Fardis, M.; McGreivy, J.; Hamdy, A.; Rothbaum, W.; Izumi, R.; Diacovo, T. G.; Johnson, A. J.; Furman, R. R. *N.*

ACCEPTED MANUSCRIPT

*Engl. J. Med.* **2016**, *374*, 323.

14. Marcotte, D. J.; Liu, Y. T.; Arduini, R. M.; Hession, C. A.; Miatkowski, K.; Wildes, C. P.; Cullen, P. F.; Hong, V.; Hopkins, B. T.; Mertsching, E.; Jenkins, T. J.; Romanowski, M. J.; Baker, D. P.; Silvian, L. F. *Protein Sci.* **2010**, *19*, 429.
15. Glide, version 5.9, Schrödinger, LLC, New York, NY, **2013**.
16. Furet, P.; Caravatti, G.; Guagnano, V.; Lang, M.; Meyer, T.; Schoepfer, J. *Bioorg. Med. Chem. Lett.* **2008**, *18*, 897.
17. Zhang, W.; Zhang, D.; Stashko, M. A.; DeRyckere, D.; Hunter, D.; Kireev, D.; Miley, M. J.; Cummings, C.; Lee, M.; Norris-Drouin, J.; Stewart, W. M.; Sather, S.; Zhou, Y.; Kirkpatrick, G.; Machius, M.; Janzen, W. P.; Earp, H. S.; Graham, D. K.; Frye, S. V.; Wang, X. *J. Med. Chem*. **2013**, *56*, 9683.
18. Harter, W. G.; Albrect, H.; Brady, K.; Caprathe, B.; Dunbar, J.; Gilmore, J.; Hays, S.; Kostlan, C. R.; Lunney, B.; Walker, N. *Bioorg. Med. Chem. Lett.* **2004**, *14*, 809.
19. Furet, P.; Bold, G.; Hofmann, F.; Manley, P.; Meyer, T.; Altmann, K. H. *Bioorg. Med. Chem. Lett.* **2003**, *13*, 2967.
20. Rapaport, D. C. (**1996**) "The Art of Molecular Dynamics Simulation". ISBN 0-521-44561-2.
21. Kumari, R.; Kumar, R.; Open Source Drug Discovery Consortium, Lynn, A. *J. Chem. Inf. Model.* **2014**, *54*, 1951.
22. Hou, T.; Wang, J.; Li, Y.; Wang, W. *J. Chem. Inf. Model.* **2010**, *51*, 69.
23. Zhu, K.; Borrelli, W. K.; Greenwood, J. R.; Day, T.; Abel, R.; Farid, R. S.; Harder, E. *J. Chem. Inf. Model.* **2014**, *54*, 1932.

ACCEPTED MANUSCRIPT

ACCEPTED MANUSCRIPT

## Graphical Abstract

To create your abstract, type over the instructions in the template box below.

**Structure-based discovery of novel 4,5,6-trisubstituted pyrimidines as potent covalent Bruton's tyrosine kinase inhibitors**

Leave this area blank for abstract info.

Yi Zou[a,‡], Jianhu Xiao[a,‡], Zhengchao Tu[b,‡], Yingyi Zhang[a], Kun Yao[a], Minghao Luo[a], Ke Ding[b,*], Yihua Zhang[a], Yisheng Lai[a,*]

[a]*State Key Laboratory of Natural Medicines, Jiangsu Key Laboratory of Drug Discovery for Metabolic Diseases, Center of Drug Discovery, China Pharmaceutical University, Nanjing 210009, PR China*

[b]*Key Laboratory of Regenerative Biology and Institute of Chemical Biology, Guangzhou Institutes of Biomedicine and Health, Chinese Academy of Sciences, Guangzhou 510530, PR China*

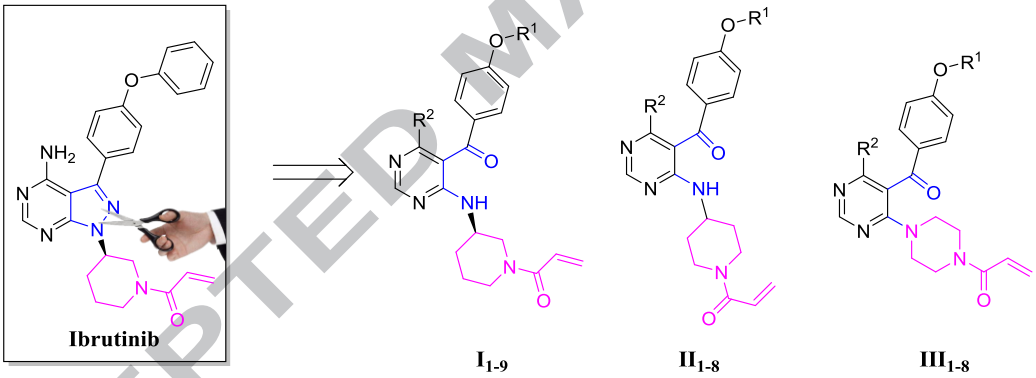


Fonts or abstract dimensions should not be changed or altered.

ACCEPTED MANUSCRIPT